

Self-Assembly | Hot Paper |

 Self-Assembled Supramolecular Hybrid Hydrogel Beads Loaded with Silver Nanoparticles for Antimicrobial ApplicationsCarmen C. Piras, Clare S. Mahon, and David K. Smith*^[a]

Abstract: This Full Paper reports the formation of silver (Ag) NPs within spatially resolved two-component hydrogel beads, which combine a low-molecular-weight gelator (LMWG) DBS-CONHNH₂ and a polymer gelator (PG) calcium alginate. The AgNPs are formed through in situ reduction of Ag^I, with the resulting nanoparticle-loaded gels being characterised in detail. The antibacterial activity of the nanocomposite gel beads was tested against two drug-resistant bac-

terial strains, often associated with hospital-acquired infections: vancomycin-resistant *Enterococcus faecium* (VRE) and *Pseudomonas aeruginosa* (PA14), and the AgNP-loaded gels showed good antimicrobial properties against both types of bacteria. It is suggested that the gel bead format of these AgNP-loaded hybrid hydrogels makes them promising versatile materials for potential applications in orthopaedics or wound healing.


Introduction


Hydrogels self-assembled from low-molecular-weight gelators (LMWGs) have seen intensive development in recent years for different types of biological applications including cell culture,^[1] tissue engineering,^[2] drug delivery,^[3] antimicrobial therapy^[4] and wound healing.^[5] These materials are obtained from the self-assembly of small molecules in water, which interact through non-covalent interactions to form complex entangled fibrillar networks.^[6] One of the most interesting properties of such gel networks is their tunability and responsiveness to external stimuli such as pH, temperature and light.^[7] However, since such gels are assembled via non-covalent interactions, they are often mechanically very weak, and can be difficult to manipulate. When designing high-tech programmable materials, spatio-temporal control over gelation to obtain spatially resolved, shaped gels is a highly desirable feature that can be achieved using different technologies including moulding, 3D printing and photopatterning.^[8] The combination of a LMWG with a polymer gelator (PG) to give a multi-component hybrid gel combines the responsiveness of the LMWG with the overall mechanical performance of the PG, potentially allowing the gels to be moulded into desired shapes.^[9] This can enable tailoring of gels for specific applications.

We recently developed a highly functional, synthetically-simple LMWG 1,3:2:4-di(4-acylhydrazide)-benzylidenesorbitol (DBS-CONHNH₂),^[10] demonstrating that this hydrogelator has potential applications ranging from environmental remediation to drug formulation and tissue engineering.^[11] This LMWG can achieve efficient reduction of precious metals, inducing the in situ formation of metal nanoparticles (NPs).^[11a,12] By combining this LMWG with the PG calcium alginate, we very recently reported that self-assembly of the LMWG could be spatially controlled by the PG to give core-shell gel beads, in which the PG shell imposes a shape on a self-assembled LMWG core.^[13] The self-assembled DBS-CONHNH₂ gel core retained its ability to generate palladium nanoparticles, and the resulting gel beads could catalyse cross-coupling reactions and operated as an efficient recyclable reaction dosage system.

To extend the potential of our innovative gel bead platform into the field of biomedicine, this paper reports the in situ formation of silver (Ag) NPs in the two-component DBS-CONHNH₂/alginate system (Figure 1). AgNPs are known to prevent biofilm formation and have antimicrobial properties against multiple drug-resistant bacterial strains.^[14] Implant-associated infections and biofilm formation on implant surfaces are common complications after orthopaedic surgery.^[15] The application of AgNPs on orthopaedic implants to avoid infections and prevent biofilm formation has recently gained some interest as an alternative to the administration of antibiotics.^[16] Furthermore, Ag can have an osteogenic effect on stem cells, promoting bone formation.^[17] Nanomaterials with antibacterial activity are an important and burgeoning field of activity.^[18] In this regard, there has been some interest in the development of supramolecular gels with embedded silver nanoparticles.^[19] In general, these have mostly been unshaped materials formed in vials. Nonetheless, there has been some investigation of the antimicrobial potential of such gels.^[20] We reasoned that the development of AgNP-loaded shapable biomaterials as bone

[a] Dr. C. C. Piras, Dr. C. S. Mahon, Prof. D. K. Smith
Department of Chemistry, University of York
Heslington, York, YO10 5DD (UK)
E-mail: david.smith@york.ac.uk

 Supporting information and the ORCID identification number(s) for the author(s) of this article can be found under:
<https://doi.org/10.1002/chem.202001349>.

 © 2020 The Authors. Published by Wiley-VCH Verlag GmbH & Co. KGaA. This is an open access article under the terms of the Creative Commons Attribution License, which permits use, distribution and reproduction in any medium, provided the original work is properly cited.

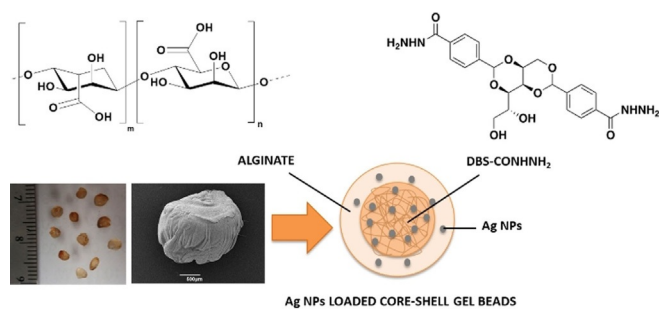


Figure 1. Structures of alginate and DBS-CONHNH₂, photograph (left) and SEM image (right) of hybrid DBS-CONHNH₂/alginate gel beads incorporating Ag NPs and schematic diagram of an AgNP-loaded core-shell gel bead.

fillers may ultimately be able to effectively help bone regeneration whilst preventing infections. Such materials could be easily handled and administered to patients as a result of the gel bead format. Indeed, bead-shaped constructs with antibacterial activity, composed of non-degradable polymers or degradable biomaterials such as calcium sulfate, are already in clinical use for treatment of bone and wound infections^[21]—our systems based on biocompatible individual components^[11c,22] and being potentially degradable soft materials, could have significant potential in this setting. As such, in this paper, we make the first report of shaped antimicrobial AgNP-loaded gel beads based on LMWG technology.

Results and Discussion

Sodium alginate and DBS-CONHNH₂ were combined as previously described by us,^[13] to give a multicomponent gel. Sodium alginate (low viscosity) is commercially available and was purchased and used as supplied. DBS-CONHNH₂ was synthesized in good yield by applying our previously reported method.^[10,23] The two networks could be spatially organised in two different ways, depending on the preparation method.

- (1) Extended interpenetrating networks were obtained by combining an aqueous suspension (1 mL final volume) of DBS-CONHNH₂ (0.3 % wt/vol) with alginate (0.5 % wt/vol). Heating ensured the complete dissolution of the LMWG and gelation was triggered on cooling. Once the DBS-CONHNH₂ gel had formed, an aqueous solution of CaCl₂ (5 % wt/vol; 1 mL) was added on top of the gel to cross-link the alginate by diffusion of calcium ions.
- (2) Core-shell structured gel beads were prepared by combining the same quantities of DBS-CONHNH₂ and alginate, but after heating, the resulting hot solution was added dropwise (20 μ L drops) to an aqueous solution of CaCl₂ (5 % wt/vol) to give small gel beads (ca. 3 mm diameter) on cross-linking of the alginate with self-assembly of the DBS-CONHNH₂ occurring simultaneously as the system cooled.

Single-component gels based on DBS-CONHNH₂ (in vials) or calcium alginate (in vials and as beads) were also prepared as control materials.

These two-component gels were previously characterised by us in detail,^[13] however as additional characterisation, we were interested here in determining whether DBS-CONHNH₂ retained the responsive properties characteristic of a supramolecular gel within our beads. We reasoned that on increasing the ambient temperature, the LMWG network within the core of the gel beads should disassemble within the calcium alginate shell. This would clearly demonstrate the dual nature of these LMWG/PG hybrids. We therefore performed a ¹H NMR spectroscopy study; this method is a powerful way of determining whether individual gelator molecules are self-assembled into “solid-like” nanofibres (and hence invisible by NMR) or are mobile within the “liquid-like” phase (in which case ¹H NMR resonances are observed).^[24] We prepared 10 gel beads in D₂O and transferred them to a NMR tube with 0.5 mL of D₂O and 2 μ L of DMSO as the internal standard. A ¹H NMR spectrum was immediately recorded to confirm that the DBS-CONHNH₂ incorporated into the gel beads was in its self-assembled state. We then heated the sample at 90 °C, and recorded the ¹H NMR spectrum at regular time intervals (Figure S1). The percentage of mobile DBS-CONHNH₂ within the gel beads was thus calculated (Figure 2, Table S1). After only 10 min at 90 °C, ca. 40% of the DBS-CONHNH₂ became mobile. This increased over time to reach ca. 75% after 8 h. It is therefore clear that although the calcium alginate provides these gel beads with their shape, the self-assembled DBS-CONHNH₂ retains its thermally responsive characteristics. This clearly indicates how using LMWG/PG hybrid gels can endow hybrid hydrogels with orthogonal properties and suggests that DBS-CONHNH₂ within the gel bead core can behave in a similar way to any other sample of this LMWG.

Having demonstrated the orthogonal nature of the LMWG/PG networks, we then went on to load these gels with silver. To trigger the in situ formation of AgNPs, gel samples were simply left to interact with AgNO₃ (1 or 3 mL of a 10 mM solution) for 3 days. The DBS-CONHNH₂ gel and the DBS-CONHNH₂/alginate hybrid gels changed colour to orange/

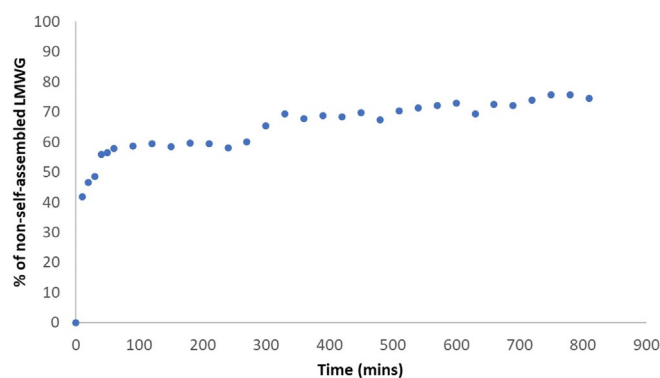


Figure 2. Overnight ¹H NMR study at 90 °C, showing the percentage of DBS-CONHNH₂ that is mobile and hence in a “liquid-like” non-self-assembled state within the gel beads.

brown as the Ag^+ ions diffused into them, clearly indicating the incorporation and in situ reduction of Ag^+ to Ag^0 (Figures S2 and S3). After 3 days, the supernatant was removed and the gels were washed with water multiple times. Transmission electron microscopy (TEM) confirmed the formation of AgNPs, with the majority of the diameters being in the range of 1–10 nm for the DBS-CONH NH_2 /alginate hybrid gels and gel beads (Figure 3, Figure S4). Control experiments with a DBS-CONH NH_2 gel indicated AgNPs with the majority of the diameters in the range of 10–30 nm (Figure S5). We observed that calcium alginate gels and gel beads could also incorporate Ag. In this case, however, the Ag-loaded alginate gel was colourless suggesting either the Ag is present in the +1 oxidation state, or that reduction to Ag^0 NPs is less effective than in the case where DBS-CONH NH_2 is present (where the gels become intensely coloured). We did observe nanoparticles in the calcium alginate gels by TEM (1–50 nm diameter), but they were irregular and tended to aggregate into significantly larger particles with a diameter > 150 nm (Figures S6 and S7). It is known that AgNPs can be formed in alginate gels, normally facilitated by heating, manipulation of pH or exposure to UV light.^[25] Indeed, silver-loaded alginate gels have been of interest in biomedical applications for their anti-microbial properties.^[26] Overall, in our hybrid hydrogels, where DBS-CONH NH_2 is present, silver uptake was significantly better controlled in terms of

nanoparticle size (Figure 4). In summary therefore, AgNPs can be incorporated into the gels—clearly facilitated by the presence of DBS-CONH NH_2 .

The incorporation of Ag into the gels was quantitatively evaluated by analysis of the remaining supernatant solution. A precipitation titration was performed in the presence of NaCl using K_2CrO_4 as an indicator. The volume of supernatant required as a titrant, was used to calculate the concentration of residual Ag in the supernatant (i.e., the Ag that was not incorporated into the gel) and, from this, the amount of Ag loaded into the gel could be determined (Table S2). When the gels were loaded with a relatively low amount of AgNO_3 (10 μmol), the DBS-CONH NH_2 gel displayed a better uptake capacity ($> 9 \mu\text{mol}$ of Ag mL^{-1} of gel) than the extended interpenetrating hybrid networks (7 μmol of Ag mL^{-1} of gel) or the hybrid gel beads (6.5 μmol of Ag mL^{-1} of gel). We suggest that this is because interactions between DBS-CONH NH_2 and alginate networks in the multicomponent gel (as previously described^[13]) somewhat limit the ability of the acylhydrazide to reduce Ag^+ to Ag^0 . However, on exposure to higher concentrations of silver (30 μmol of AgNO_3), we were able to maximise the uptake of silver. For the interpenetrating network hybrid gel, we could achieve a maximum of 15 μmol of Ag mL^{-1} of gel. When the gel was prepared as hybrid gel beads, the maximum uptake was slightly higher (18 μmol of Ag mL^{-1} of gel) possibly due to the larger surface area of the beads. The hybrid gel contains 6.3 μmol of DBS-CONH $\text{NH}_2 \text{ mL}^{-1}$, and these data therefore indicate that the gelator can take up approximately 2–3 equivalents of Ag. In general, gels composed only of calcium alginate also took up a similar amount of Ag to the gels containing DBS-CONH NH_2 , however, as described above there was much less control over AgNP formation.

The macroscopic performance of the Ag-loaded gels was then determined. For practical reasons, these experiments were conducted on the extended interpenetrating network hybrid gels. The thermal stability was measured as the gel-sol transition temperature (T_{gel}) using a simple tube inversion method (Table S3). The T_{gel} of the DBS-CONH NH_2 gel (0.4% wt/vol) is 86 °C, but in the presence of increasing Ag loading (10 and 30 μmol of AgNO_3 added on top of the gel), the T_{gel} value decreased to 37 and 30 °C respectively. This indicates that the presence of AgNPs disrupts the fibre-fibre interactions. By contrast, the T_{gel} values of the DBS-CONH NH_2 /alginate hybrid gels

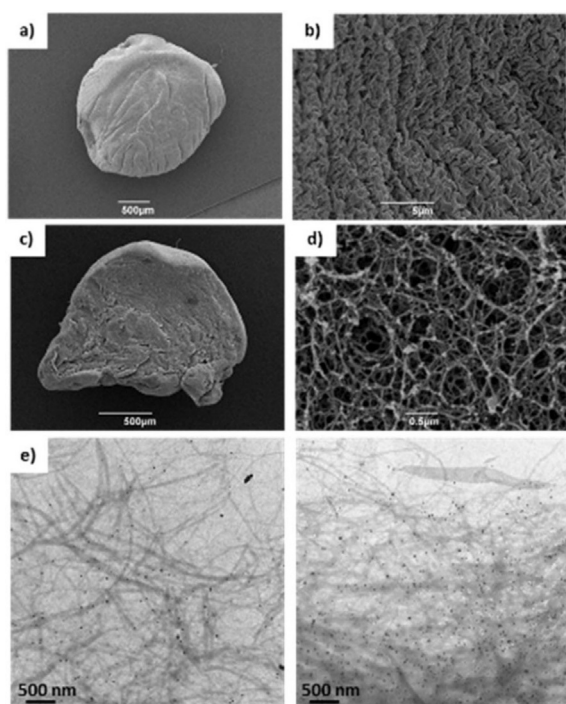


Figure 3. SEM and TEM images of DBS-CONH NH_2 /alginate gel beads incorporating AgNPs and TEM images of DBS-CONH NH_2 gel incorporating AgNPs. a) SEM image of a DBS-CONH NH_2 /alginate gel bead (scale bar 500 μm); b) SEM image of DBS-CONH NH_2 /alginate gel bead surface (scale bar 5 μm); c) SEM image of a cross section of a DBS-CONH NH_2 /alginate gel bead (scale bar 500 μm); d) SEM image of a cross-section of a DBS-CONH NH_2 /alginate gel bead (scale bar 0.5 μm). e) TEM images of DBS-CONH NH_2 /alginate gel bead cross-section (scale bars 500 nm). SEM images of the gels with no Ag NPs are reported in the Supporting Information (Figures S8 and S9).

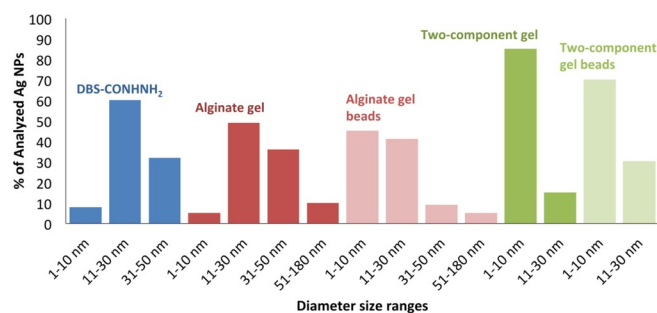


Figure 4. Ag NPs diameter size ranges in DBS-CONH NH_2 , alginate gels and gel beads and DBS-CONH NH_2 /alginate gels and gel beads.

(0.3% wt/vol of DBS-CONHNH₂ and 0.5% wt/vol of alginate) and of the alginate gel (0.8% wt/vol) were above 100 °C both in the absence and presence of AgNPs, indicating that the presence of the PG network increases the thermal stability of the gel, which is therefore, macroscopically not affected by the presence of AgNPs in the analysed temperature range (25–100 °C).

The mechanical properties of the Ag-loaded gels were studied by oscillatory rheology using a parallel plate geometry (Table 1, Figure S10–S18). The DBS-CONHNH₂ hydrogel (0.4% wt/vol) has an elastic modulus (G') of 800 Pa, which in the presence of increasing Ag loadings (10 and 30 μmol of AgNO₃ added on top of the gels) decreases approximately 200-fold to around 4 Pa to give a very soft gel indeed. This supports the T_{gel} data and is in-line with the view that AgNPs disrupt fibre-fibre interactions due to the close proximity of the NPs to the gel fibres, thus reducing gel stiffness. On the other hand, the DBS-CONHNH₂/alginate hybrid gel (0.3% wt/vol of DBS-CONHNH₂ and 0.5% wt/vol of alginate) displayed higher G' values with increasing Ag loading (G' increased from 8030 to 13 800 Pa). This is probably because the presence of the PG dominates the rheological performance of the gel and therefore in this case, the AgNPs simply mechanically reinforce the gel rather than disrupting it. Indeed, a similar trend was seen when testing the calcium alginate gel alone. It is well known, in general terms, that nanoparticle additives can toughen soft materials.^[27] Overall, for the LMWG-containing gels, as is often observed, gel stiffness is broadly inversely correlated with resistance to shear strain (as reflected in the G'/G'' crossover point).

Most importantly, having developed and characterised AgNP-loaded gels, we wanted to demonstrate that they display antimicrobial properties. We therefore performed a disc diffusion assay, testing the gels against two different bacterial strains: vancomycin-resistant *Enterococcus faecium* (VRE), a Gram-positive bacterium resistant to the antibiotic vancomycin,^[28] and *Pseudomonas aeruginosa* (PA14), a Gram-negative bacterium.^[29] These bacterial strains are often associated with hospital-acquired infections in immuno-compromised individuals such as hospitalised patients in intensive care units, pa-

tients with cancer, receiving dialysis or who have had a transplant. The test was performed by placing AgNP-loaded gels on an agar plate where the bacteria were cultured (section S8, Supporting Information). The plates were left to incubate for 24 hours and, after this time, the zones of inhibition were measured.

Pleasingly, all of the gels loaded with AgNPs showed good antibacterial performance with zones of inhibition between 2 and 3 mm (Figure 5, top), comparable to previous results in the literature for AgNP-loaded hydrogels.^[20] In contrast, gels without AgNPs showed no activity (Figure 5, bottom). Importantly, the hybrid gel beads showed similar activity to the extended interpenetrating network gels (Tables S4 and S5). These results therefore clearly demonstrate that antimicrobial performance can be achieved by the shaped hybrid gel system. These are promising preliminary results, which demonstrate that the AgNP hybrid hydrogel beads have antibacterial properties against both Gram-positive and Gram-negative drug-resistant bacteria. We reason that the gel beads may be particularly appropriate for use in wound healing settings or after surgical intervention, as a result of their ease of handling.

There has been debate over the antimicrobial mode of action of silver nanoparticles.^[30] It has been noted that Ag^I ions have antimicrobial properties, but also that AgNPs have distinct mechanisms of action. We therefore determined the extent of Ag^I release from AgNP-loaded gel beads in order to better understand whether silver ions were released. This was quantitatively evaluated by suspending the beads in water, and analysing the solution for Ag^I using a precipitation titra-

Table 1. Rheological data as determined by using oscillatory rheometry with a parallel plate geometry, for DBS-CONHNH₂ gels, calcium alginate gels, and interpenetrated network gels formed by the combination of the two. Loadings are given in wt/vol, and the G'/G'' crossover points ($G' = G''$) refer to the % shear strain at which $G' = G''$.

Gel	LMWG loading (wt/vol)	PG loading (wt/vol)	Ag loading [μmol]	G' [Pa]	$G' = G''$ (shear strain)
LMWG	0.4%	–	–	800	25.1%
LMWG	0.4%	–	10	3.68	39.7%
LMWG	0.4%	–	30	4.13	31.5%
PG	–	0.8%	–	2500	2.3%
PG	–	0.8%	10	3000	1.6%
PG	–	0.8%	30	6000	2.1%
LMWG/PG	0.3%	0.5%	–	8030	3.8%
LMWG/PG	0.3%	0.5%	10	8480	3.6%
LMWG/PG	0.3%	0.5%	30	13 800	3.5%

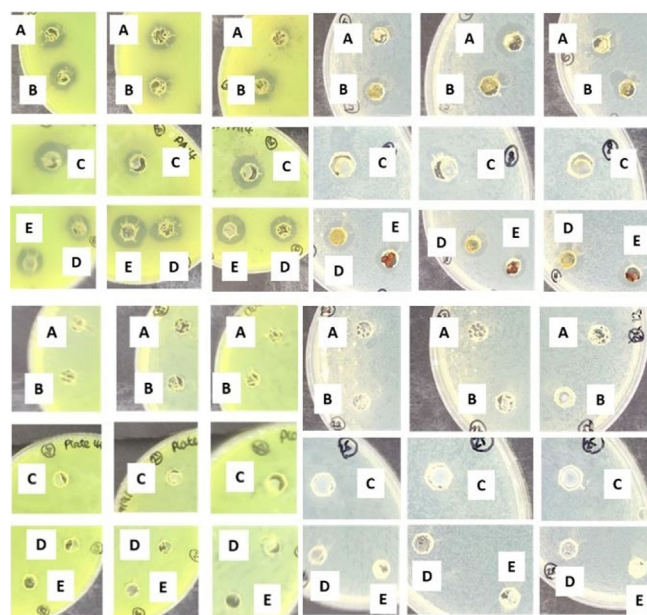


Figure 5. Photographic images of the disc diffusion assay. (Left) *Pseudomonas aeruginosa* (PA14). (Right) Vancomycin resistant *Enterococcus faecium* (VRE). (Top) Gels loaded with AgNPs, the dark rings indicate the zone of inhibition. (Bottom) Control gels without AgNPs. (A) Alginate gel, (B) alginate gel beads, (C) DBS-CONHNH₂/alginate gel, (D) DBS-CONHNH₂/alginate gel beads, (E) DBS-CONHNH₂ gel. Water, kanamycin and vancomycin controls have been reported in the Supporting Information (Figures S19 and S20).

tion in the presence of NaCl and using K_2CrO_4 as an indicator. Studies were performed in triplicate (Tables S6 and S7). It was evident that a small amount of Ag^I (ca. 20%) is initially released from the gel, but after 30 minutes no further silver ions are released (Figure 6). After 24 h, the release medium was replaced with fresh water, and no further release of silver ions was observed. This would suggest that any longer term antimicrobial activity associated with these gel beads is more likely associated with slow AgNP release or the production of reactive oxygen species by AgNPs embedded within the gels. Further studies to understand such effects will be carried out in the future as these biomaterials are translated into a more applied setting.

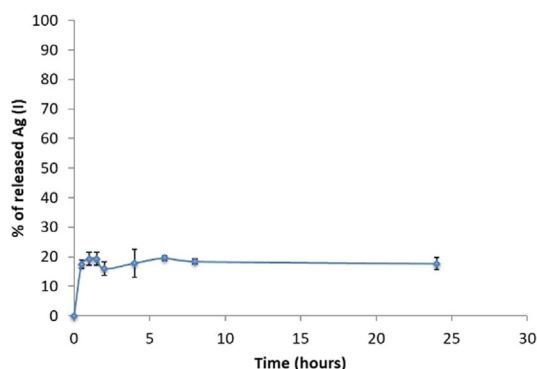


Figure 6. Release over time of Ag^I ions from the DBS-CONH₂/alginate hybrid gel beads.

Conclusions

In conclusion, we have shown that in our two-component DBS-CONH₂/alginate gel system that can be formulated as hybrid gel beads, both the LMWG and PG networks retains some of their key functions. The self-assembled LMWG network remains thermally responsive within the hybrid gel beads, and is capable of generating AgNPs through in situ reduction of Ag^I to Ag^0 , providing excellent size control over the resulting nanoparticles. The alginate PG mechanically reinforces the gels and enables shaping of these materials into core-shell beads. In a standard DBS-CONH₂ gel, the presence of AgNPs disrupts fibre-fibre interactions, reducing gel thermal stability and adversely affecting mechanical properties. In contrast, once calcium alginate is present in the multicomponent gel, the thermal stability remains high and gel stiffness is actually increased by AgNPs, suggesting the PG dominates the rheological performance. Once again this demonstrates the synergistic characteristics of the hybrid LMWG/PG gel. Initial screening of the AgNP-loaded gels showed very good antimicrobial properties against drug-resistant bacteria, in particular, VRE and *P. aeruginosa*. Furthermore, given that the individual components of the hybrid LMWG/PG gel beads are biocompatible,^[11c,22] we believe that these DBS-CONH₂/alginate gels could be promising biocompatible materials.

In summary, we note that the combination of LMWG and PG reported in this paper enables:

1. Excellent control over AgNP size (because of the LMWG),
2. Improved mechanical properties (because of the PG),
3. Ability to shape the active LMWG into a core-shell bead format (because of the PG).

We suggest that these gel beads, which are very easy to handle and manipulate, and have antimicrobial properties against drug-resistant bacteria, may be promising materials for orthopaedic applications or wound healing, particularly given that antibacterial bead-shaped constructs are already in widespread clinical use in this setting.^[21] Further studies in this direction are in progress.

Acknowledgements

We acknowledge EPSRC (CCP and DKS: EP/P03361X/1) and the European Commission Marie Curie IF Scheme (CSM: 702927). We thank H. Fish for the overnight NMR study (Department of Chemistry, University of York) and M. Stark (Bioscience Technology Facility, Department of Biology, University of York) for SEM and TEM imaging.

Conflict of interest

The authors declare no conflict of interest.

Keywords: antimicrobial · gel · nanoparticle · self-assembly · supramolecular chemistry

- [1] X. Q. Dou, C. L. Feng, *Adv. Mater.* **2017**, *29*, 1604062.
- [2] a) L. Saunders, P. X. Ma, *Macromol. Biosci.* **2019**, *19*, 1800313; b) J. Hoque, N. Sangaj, S. Varghese, *Macromol. Biosci.* **2019**, *19*, 1800259.
- [3] a) M. C. I. M. Amin, N. Ahmad, M. Pandey, M. M. Abeer, N. Mohamad, *Exp. Opin. Drug Deliv.* **2015**, *12*, 1149–1161; b) M. R. Saboktakin, R. M. Tabatabaei, *Int. J. Biol. Macromol.* **2015**, *75*, 426–436.
- [4] a) A. M. Carmona-Ribeiro, *Int. J. Environ. Res. Public Health* **2018**, *15*, 1408; b) B. Hu, C. Owh, P. L. Chee, W. R. Leow, X. Liu, Y. L. Wu, P. Guo, X. J. Loh, X. Chen, *Chem. Soc. Rev.* **2018**, *47*, 6917–6929.
- [5] a) Z. Yang, G. Liang, M. Ma, A. S. Abbah, W. W. Lu, B. Xu, *Chem. Commun.* **2007**, 843–845; b) Z. Zhai, K. Xu, L. Mei, C. Wu, J. Liu, Z. Liu, L. Wan, W. Zhong, *Soft Matter* **2019**, *15*, 8603–8610.
- [6] a) X. Du, J. Zhou, J. Shi, B. Xu, *Chem. Rev.* **2015**, *115*, 13165–13307; b) E. R. Draper, D. J. Adams, *Chem* **2017**, *3*, 390–410.
- [7] C. D. Jones, J. W. Steed, *Chem. Soc. Rev.* **2016**, *45*, 6546–6596.
- [8] P. R. A. Chivers, D. K. Smith, *Nat. Rev. Mater.* **2019**, *4*, 463–478.
- [9] D. J. Cornwell, D. K. Smith, *Mater. Horiz.* **2015**, *2*, 279–293.
- [10] B. O. Okesola, D. K. Smith, *Chem. Commun.* **2013**, *49*, 11164–11166.
- [11] a) B. O. Okesola, S. K. Suravaram, A. Parkin, D. K. Smith, *Angew. Chem. Int. Ed.* **2016**, *55*, 183–187; *Angew. Chem.* **2016**, *128*, 191–195; b) P. R. A. Chivers, D. K. Smith, *Chem. Sci.* **2017**, *8*, 7218–7227; c) V. M. P. Vieira, A. C. Lima, M. de Jong, D. K. Smith, *Chem. Eur. J.* **2018**, *24*, 15112–15118; d) C. C. Piras, D. K. Smith, *Chem. Eur. J.* **2019**, *25*, 11318–11326.
- [12] P. Slavik, D. W. Kurka, D. K. Smith, *Chem. Sci.* **2018**, *9*, 8673–8681.
- [13] C. C. Piras, P. Slavik, D. K. Smith, *Angew. Chem. Int. Ed.* **2020**, *59*, 853–859; *Angew. Chem.* **2020**, *132*, 863–869.
- [14] a) N. Durán, M. Durán, M. B. de Jesus, A. B. Seabra, W. J. Fávaro, G. Nakazato, *Nanomedicine* **2016**, *12*, 789–799; b) M. Bilal, T. Rasheed, H. M. N. Iqbal, H. Hu, X. Zhang, *Int. J. Pharmacol.* **2017**, *13*, 832–845; c) K. C. Hembram, R. Kumar, L. Kandha, P. K. Parhi, C. N. Kundu, B. K. Bindhani, *Artif. Cells, Nanomed. Biotechnol.* **2018**, *46*, S38–S51; d) K. Kalwar, D. Shan, *Micro Nano Lett.* **2018**, *13*, 277–280; e) P. Prasher, M. Singh, H. Mudila, *3 Biotech* **2018**, *8*, e411; f) F. Paladini, M. Pollini, *Materials* **2019**,

- 12, 2540; g) A. Roy, O. Bulut, S. Some, A. K. Mandal, M. D. Yilmaz, *RSC Adv.* **2019**, *9*, 2673–2702; h) S. Some, I. Kumar Sen, A. Mandal, T. Aslan, Y. Ustun, E. Ş. Yilmaz, A. Kati, A. Demirbas, A. K. Mandal, I. Ocsy, *Mater. Res. Express* **2019**, *6*, 012001.
- [15] a) M. Ribeiro, F. J. Monteiro, M. P. Ferraz, *Biomatter* **2012**, *2*, 176–194; b) Z. Khatoun, C. D. McTiernan, E. J. Suuronen, T.-F. Mah, E. I. Alarcon, *Heliyon* **2018**, *4*, e01067; c) M. Wang, T. Tang, *J. Orthopaed. Translat.* **2019**, *17*, 42–54.
- [16] a) S. A. Brennan, C. N. Fhoghlú, B. M. DeVitt, F. J. O'Mahony, D. Brabazon, A. Walsh, *Bone Joint J.* **2015**, *97*, 582–589; b) Y. A. Qing, L. Cheng, R. Li, G. Liu, Y. Zhang, X. Tang, J. Wang, H. Liu, Y. Qin, *Int. J. Nanomed.* **2018**, *13*, 3311–3327.
- [17] L.-L. Li, H.-W. An, B. Peng, R. Zheng, H. Wang, *Mater. Horiz.* **2019**, *6*, 1794–1811.
- [18] a) H. Basit, A. Pal, S. Sen, S. Bhattacharya, *Chem. Eur. J.* **2008**, *14*, 6534–6545; b) M. O. M. Piepenbrock, N. Clarke, J. W. Steed, *Soft Matter* **2011**, *7*, 2412–2418; c) J. L. Li, X.-Y. Liu, X.-G. Wang, R.-Y. Wang, *Langmuir* **2011**, *27*, 7820–7827; d) J. Nanda, B. Adhikari, S. Basak, A. Banerjee, *J. Phys. Chem. B* **2012**, *116*, 12235–12244; e) M. Maity, V. S. Sajisha, U. Maitra, *RSC Adv.* **2015**, *5*, 90712–90719; f) C. Narayana, R. K. Upadhyaya, R. Chaturvedi, R. Sagar, *New J. Chem.* **2017**, *41*, 2261–2267; g) R. Tatkonda, K. Bertula, Nonappa, S. Hietala, K. Rissanen, M. Haukka, *Dalton Trans.* **2017**, *46*, 2793–2802; h) S. Paul, K. Basu, K. S. Das, A. Banerjee, *ChemNanoMat* **2018**, *4*, 882–887; i) T. Kar, N. Patra, *J. Phys. Org. Chem.* **2020**, *33*, e4026.
- [19] a) A. Shome, S. Dutta, S. Maiti, P. K. Das, *Soft Matter* **2011**, *7*, 3011–3022; b) Y. Wang, L. Cao, S. Guan, G. Shi, Q. Luo, L. Miao, I. Thistlethwaite, Z. Huang, J. Xu, J. Liu, *J. Mater. Chem.* **2012**, *22*, 2575–2581; c) S. K. Mandal, S. Brahmachari, P. K. Das, *ChemPlusChem* **2014**, *79*, 1733–1746; d) M. R. Reithofer, A. Lakshmanan, A. T. K. Ping, J. M. Chin, C. A. E. Hauser, *Biomaterials* **2014**, *35*, 7535–7542; e) T. Simon, C.-S. Wu, J.-C. Liang, C. Cheng, F.-H. Ko, *New J. Chem.* **2016**, *40*, 2036–2043; f) Y. Niu, T. Guo, X. Yuan, Y. Zhao, L. Ren, *Soft Matter* **2018**, *14*, 1227–1234; g) F. Paladini, S. T. Meikle, I. R. Cooper, J. Lacey, V. Perugini, M. Santin, *J. Mater. Sci. Mater. Med.* **2013**, *24*, 2461–2472; h) J. Li, R. Xing, S. Bai, X. Yan, *Soft Matter* **2019**, *15*, 1704–1715; i) J. Song, C. Yuan, T. Jiao, R. Xing, M. Yang, D. J. Adams, X. Yan, *Small* **2020**, *16*, 1907309.
- [20] a) X. Liu, W. He, Z. Fang, A. Kienzle, Q. Feng, *J. Biomed. Nanotechnol.* **2014**, *10*, 1277–1285; b) B. Tian, W. Chen, Y. Dong, J. V. Marymont, Y. Lei, Q. Ke, Y. Guo, Z. Zhu, *RSC Adv.* **2016**, *6*, 8549–8562; c) S. Castiglioni, A. Cazzaniga, L. Locatelli, J. A. M. Maier, *Nanomaterials* **2017**, *7*, 124; d) X. Li, H. Bai, Y. Yang, J. Yoon, S. Wang, X. Zhang, *Adv. Mater.* **2019**, *31*, 1805092.
- [21] a) K. Klemm, *Clin. Microbiol. Infect.* **2001**, *7*, 28–31; b) D. Campoccia, L. Montanaro, P. Speziale, C. R. Aricola, *Biomaterials* **2010**, *31*, 6363–6377; c) T. A. G. van Vugt, J. J. Arts, J. A. P. Geurts, *Front. Microbiol.* **2019**, *10*, 1626.
- [22] a) T. Andersen, P. Auk-Emblem, M. Dornish, *Microarrays* **2015**, *4*, 133–161; b) A. C. Hernández-González, L. Téllez-Jurado, L. M. Rodríguez-Lorenzo, *Carbohydr. Polym.* **2020**, *229*, 115514; c) L. Bedian, A. M. Villalba-Rodríguez, G. Hernández-Vargas, R. Parra-Saldivar, H. M. N. Iqbal, *Int. J. Biol. Macromol.* **2017**, *98*, 837–846.
- [23] D. J. Cornwell, B. O. Okesola, D. K. Smith, *Soft Matter* **2013**, *9*, 8730–8736.
- [24] a) B. Escuder, M. Llusar, J. F. Miravet, *J. Org. Chem.* **2006**, *71*, 7747–7752; b) A. R. Hirst, J. F. Miravet, B. Escuder, L. Noirez, V. Castelletto, I. W. Hamley, D. K. Smith, *Chem. Eur. J.* **2009**, *15*, 372–379.
- [25] a) E. Torres, Y. N. Mata, M. L. Blázquez, J. A. Muñoz, F. González, A. Ballester, *Langmuir* **2005**, *21*, 7951–7958; b) J. Yang, H. Zheng, S. Han, Z. Jiang, X. Chen, *RSC Adv.* **2015**, *5*, 2378–2382; c) S. V. Kapranov, V. I. Ryabushko, *J. Nanopart. Res.* **2018**, *20*, e275; d) Y. Shao, C. Wu, T. Wu, C. Yuan, S. Chen, T. Ding, X. Ye, Y. Hu, *Int. J. Biol. Macromol.* **2018**, *111*, 1281–1292.
- [26] a) M. Omidkhoda, N. Hasanzadeh, F. Soleimani, H. Shafaei, *Dental Res. J.* **2019**, *16*, 372–376; b) J. Stojkowska, Z. Djurdjevic, I. Jancic, B. Bufan, M. Milenkovic, R. Jankovic, V. Miskovic-Stankovic, B. Obradovic, *J. Biomater. Appl.* **2018**, *32*, 1197–1211; c) H. Zhang, M. Peng, T. Cheng, P. Zhao, L. Qiu, J. Zhou, G. Lu, J. Chen, *J. Mater. Sci.* **2018**, *53*, 14944–14952.
- [27] a) J. Nanda, A. Biswas, B. Adhikari, A. Banerjee, *Angew. Chem. Int. Ed.* **2013**, *52*, 5041–5045; *Angew. Chem.* **2013**, *125*, 5145–5149; b) P. Thoniyot, M. J. Tan, A. A. Karim, D. J. Young, X. J. Loh, *Adv. Sci.* **2015**, *2*, 1400010; c) S. Grijalvo, R. Eritja, D. D. Díaz, *Gels* **2019**, *5*, 24.
- [28] a) K. Reyes, A. C. Bardossy, M. Zervos, *Infectious Dis. Clin. N. Am.* **2016**, *30*, 953–965; b) M. Alevizakos, A. Gaitanidis, D. Nasioudis, K. Tori, M. E. Flokas, E. Mylonakis, *Open Forum Infect. Dis.* **2017**, *4*, ofw246; c) M. E. Flokas, S. A. Karageorgos, M. Detsis, M. Alevizakos, E. Mylonakis, *Int. J. Antimicrob. Agents* **2017**, *49*, 565–572; d) H. McDermott, M. Skally, J. O'Rourke, H. Humphreys, D. Fitzgerald-Hughes, *Infect. Control Hosp. Epidemiol.* **2018**, *39*, 40–45; e) M. O. Ahmed, K. E. Baptiste, *Microb. Drug Resist.* **2018**, *24*, 590–606.
- [29] a) F. Javanmardi, A. Emami, N. Pirbonyeh, A. Keshavarzi, M. Rajaei, *Infect. Genet. Evol.* **2019**, *75*, 104037; b) P. Pachori, R. Gothwal, P. Gandhi, *Genes Dis.* **2019**, *6*, 109–119; c) Z. Pang, R. Raudonis, B. R. Glick, T. J. Lin, Z. Cheng, *Biotechnol. Adv.* **2019**, *37*, 177–192; d) A. Rojas, Z. R. Palacios-Baena, L. E. López-Cortés, J. Rodríguez-Baño, *Clin. Microbiol. Infect.* **2019**, *25*, 964–970.
- [30] a) J. A. Lemire, J. J. Harrison, R. J. Turner, *Nat. Rev. Microbiol.* **2013**, *11*, 371–384; b) T. C. Dakal, A. Kumar, R. S. Majumdar, V. Yadav, *Front. Microbiol.* **2016**, *7*, 1831; c) Y. Dong, S. Sun, *Curr. Pharmacol. Rep.* **2019**, *5*, 401–419.

Manuscript received: March 18, 2020

Revised manuscript received: April 8, 2020

Accepted manuscript online: April 15, 2020

Version of record online: June 11, 2020